Chemical Fixation Creates Nanoscale Clusters on the Cell Surface by Aggregating Membrane Proteins

Takehiko Ichikawa (tichikawa@staff.kanazawa-u.ac.jp)
Kanazawa University https://orcid.org/0000-0002-2438-5502

Dong Wang
WPI Nano Life Science Institute (WPI-NanoLSI), Kanazawa University

Keisuke Miyazawa
Kanazawa University

Kazuki Miyata
Kanazawa University https://orcid.org/0000-0002-1641-2160

Masanobu Oshima
Cancer Research Institute, Kanazwa University https://orcid.org/0000-0002-3304-0004

Takeshi Fukuma
Kanazawa University https://orcid.org/0000-0001-8971-6002

Article

Keywords: Chemical fixation, protein, nanoscale artefact, microporous silicon nitride

Posted Date: October 11th, 2021

DOI: https://doi.org/10.21203/rs.3.rs-954703/v1

Version of Record: A version of this preprint was published at Communications Biology on May 20th, 2022. See the published version at https://doi.org/10.1038/s42003-022-03437-2.

Abstract

Chemical fixations have been thought to preserve the structures of the cells or tissues. However, given that the fixatives create crosslinks or aggregate proteins, there is a possibility that these fixatives create nanoscale artefacts by aggregation of membrane proteins which move around freely to some extent on the cell surface. Despite this, little research has been conducted about this problem, probably because there has been no method for observing cell surface structures at the nanoscale. In this study, we have developed a new method to observe cell surfaces stably and with high resolution using atomic force microscopy and a microporous silicon nitride membrane. We demonstrate that the size of the protrusions on the cell surface is increased after treatment with three commonly used fixatives and show that these protrusions were created by the aggregation of membrane proteins by fixatives. These results call attention when observing fixed cell surfaces at the nanoscale.

Introduction

Fixation of cells or tissues is the critical first step for histochemical or cytochemical investigations, and thousands of studies have adopted this method for their research[1, 2, 3]. Of commonly used chemical fixatives, aldehyde fixatives such as paraformaldehyde (PFA) and glutaraldehyde (GA) create crosslinking between neighbouring proteins, and alcohol fixatives such as methanol (MeOH) fix tissues by dehydration[4, 5, 6, 7, 8, 9]. Given this mechanism, it has been speculated that proteins on the cell membrane can move freely to some extent aggregate during the fixation process[10, 11]. This has a possibility to cause artefacts by creating pseudo-clusters. Previous studies reported that fixatives can change a part of the cell surface structures at scales of hundreds of nanometers to microns. However, no reports investigated surface structures on mammalian cells with a resolution of several nanometers[12, 13, 14, 15, 16, 17, 18, 19, 20, 21, 22, 23, 24, 25], because it is still difficult to observe living cell surface at several nanometer scales.

So far, many investigations of the cell surface have been performed using optical microscopes or electron microscopes. Optical microscopes are possible to observe the living cell, but the special resolution is more than 200 nm due to the diffraction limit. Even the recently developed super-resolution techniques have a special resolution of 10 - 100 nm, and still not possible to observe a few nanometer structures. On the other side, electron microscopes have a high special resolution of less than 1 nm, but these cannot observe the living samples. Atomic force microscopy (AFM) has a high special resolution of less than 1 nm, and this is applicable to the living cell observation[26, 27, 28, 29, 30]. However, cell surface molecules have been observed using AFM only on the bacterial cells, which have a relatively hard cell wall, and it has been difficult to image the surface of mammalian cells, probably because its surface is soft and moving dynamically[30, 31, 32, 33, 34, 35, 36, 37, 38]. In this study, to overcome this difficulty in the observation of mammalian cells using AFM, we developed a method using microporous silicon nitride membrane (MPM) and successfully observed sub-10 nm protrusions on the cell surface that are comparable to the single molecule[39, 40, 41]. Using this method, we report that the size of the protrusions on the cell surface increased after treatment with commonly used chemical fixation methods, probably because of the

aggregation of membrane proteins. These results indicate that chemical fixation creates nanoscale aggregations on the cell surface.

Results

A new method for high-resolution observation of living cell surface using atomic force microscopy

To achieve the nanoscale AFM imaging of the cell surface, we developed a new method using commercially available MPM as a sample holder of the transmission electron microscope (https://www.norcada.com/products/porous-membranes). We used a 0.2 μm-thick MPM with 5 μm holes at 10 μm pitch supported by a silicon frame sized of 2.6 × 2.6 × 0.2 mm (Figure 1a - c). We placed the MPM on a 35 mm plastic dish using double-sided tape for the membrane side facing down and cultured human colon cancer DLD-1 cells on the backside of the membrane (Figure 1f). We confirmed that DLD-1 cell normally grows on MPM (Figure 1d). Next, we fixed the cell-cultured MPM on the custom-made holder implemented with a perfusion system for the membrane side facing up (Figure 1f and g) and then observed the cell surface with AFM through a hole in the MPM (Figure 1h). By supporting the cell membrane around the observation area with the MPM, we expected this method would reduce the surface fluctuation, making it possible to perform stable and high-resolution imaging on the cell surface using AFM.

The results of the AFM observation of the living DLD-1 cell surface using MPM are shown in Figure 2a-c. Large-scale image (Figure 2a; 2.5 × 2.5 μm), intermediate-scale image (Figure 2b; 0.5 × 0.5 μm), and the same position of three consecutive small-scale images (Figure 2c; 100 × 100 nm) acquired every 2 min are shown. The protrusions marked by arrowheads of the same colour in Figure 2c indicate the same protrusions, which means that these protrusions are not artefacts by AFM but real structures. To quantify the size of the protrusions, we developed an auto-recognition tool using MATLAB (Supplementary Figure 1). Figure 2d shows the boundary of the recognized area overlaid on the third image in Figure 2c. The distributions of the measured area and the nearest distance between protrusions are shown in Figure 2u and v. Figure 2e shows the height profile measured along the line in Figure 2c. The half-width at half maximum (HWHM) was measured as 6.3 nm (left) and 5.38 nm (right). This size is comparable to the size of a single membrane protein[39, 40, 41]. From these results, we are able to observe single-molecule scale structures on the surface of living cells by using MPM and AFM.

Commonly used fixatives create large protrusions on the cell surface

The results of the AFM observations after treatment with three popular fixatives are presented in Figure 2f and later. Figures 2f-j show the results after treatment with 4% PFA for 30 min at room temperature (RT). Large (2.5 × 2.5 μm), intermediate (0.5 × 0.5 μm), and small scale (100 × 100 nm) of AFM images are shown in Figure 2f-h, respectively. Figure 2i is the boundary of the protrusion superimposed image in the

third image of Figure 2h. The size of the protrusions appears to be larger than that of the living cell in Figure 2d. The height profile measured along the line in Figure 2h is shown in Figure 2j, and the HWHM was measured as 11.9 nm, which is approximate twice the size of the living protrusions in Figure 2e. Figure 2k-o show the results after treatment with 2% GA for 1 h at RT. The HWHM in Figure 2o, the heigh profile along the line in Figure 2m is 9.3 nm. Figure 2p-t depicts the results after treatment with cold 100% MeOH at −20°C. The HWHM in Figure 2t, the height profile along the line in Figure 2r is 16.1 nm. Mean values (± standard error of the mean, SEM) of the size of the protrusions in Figure 2u indicated with red lines are 120.1 ± 12.32 (living), 226 ± 31.31 (PFA), 268.1 ± 25.35 (GA), and 238.9 ± 21.35 (MeOH) nm^2. All fixatives significantly increased the size of the protrusions. The mean values (± SEM) of the nearest distances between protrusions in Figure 2v were 18.09 ± 0.41 (living), 25.34 ± 0.73 (PFA), 27.44 ± 0.89 (GA), 20.39 ± 0.58 (MeOH) nm. These results demonstrate that the distances between protrusions are significantly increased after treatment with the three fixatives. These results suggest that the fixatives make large protrusions by aggregating mobile membrane proteins and, therefore, there are only large protrusions on the cell surface, and the distances between prolusions were increased.

Chemical fixation is known to increase the elasticity of the cell surface[18, 42, 43, 44]. To confirm that chemical fixation was effective in our system, we measured Young's modulus of the cell surface before and after the fixative treatment (Supplementary Figure 2). We estimated Young's modulus by fitting the Hertz-Sneddon model[45, 46] to the approaching force-distance curves at each XY position. The average values of Young's modulus ± SEM of cell surface were as 27.21 ± 5.43 (living), 449 ± 65.46 (PFA), 534.8 ± 49.7 (GA) and 165.3 ± 11.64 kPa (MeOH). Thus, all the fixatives used increased Young's modulus by 6 - 20 times, which is consistent with previous results[18, 20, 43, 44, 47].

Fluorescence experiments show that the fixatives decrease the nearest distances between irrelevant molecules

To investigate the possibility that the increased size of the protrusions observed after the fixative treatment was caused by the aggregation of membrane proteins, we used confocal fluorescence microscopy and measured the nearest distances between irrelevant molecules, E-cadherin and the epithelial cell adhesion molecule EpCAM (CD326). These molecules are highly expressed in many cells, and they are reported not to bind each other through direct binding experiments[48]. We labelled E-cadherin and EpCAM using antibodies that bind to extracellular domains and fluorescence-labelled secondary antibodies. Figure 3a shows images before and after PFA treatment. We quantified the positions of the spots and measured the nearest distances from E-cadherin to EpCAM (Figure 3b). We aligned the number of spots before and after fixation to avoid changing the area per spot. Mean values ± SEM before and after PFA treatment are 0.67 ± 0.06 and 0.48 ± 0.04 μm, respectively. The nearest distances between E-cadherin and EpCAM were significantly decreased after PFA treatment ($p < 0.01$, t-test).

Figure 3c shows the results for the GA treatment. The mean values ± SEM before and after GA treatment are 0.63 ± 0.05 and 0.41 ± 0.02 μm, respectively (Figure 3d). The nearest distances are significantly decreased after GA treatment ($p < 0.001$). Figure 3e shows the results of the MeOH treatment. The mean

values ± SEM before and after MeOH treatment are 0.46 ± 0.03 and 0.37 ± 0.04 μm, respectively (Figure 3f). The nearest distances significantly decreased after MeOH treatment, but the effect was weaker than PFA or GA ($p < 0.05$). Lastly, we observed the movement of membrane molecules during fixation. Figure 3g shows the time series during fixation when GA was added at the 0-time point. After adding GA, the E-cadherin (red) spot moved around for approximately 10 s and then stopped by aggregating with the EpCAM molecule. Figure 3h shows the time-lapse change of the distance from the indicated E-cadherin to nearest EpCAM in Figure 3g. Before adding the fixative, the nearest distance fluctuated by repeating approaching and separating. After adding the fixative, the nearest distance was set to a low value after approximately 10 s. Figure 3i shows a model of the behaviour of membrane proteins before and after fixation. Before adding fixatives, membrane proteins repeat the approach or move away from each other (left). However, after adding a fixative, it becomes difficult for the proteins to move away from each other once they make contact (right). Membrane proteins rapidly create clusters through the incorporation of the free-moving molecules. As a result, large protrusions are formed on the cell surface, and the mean nearest distance between molecules decreases.

The positions of the membrane proteins in the fluorescence image are on the large protrusion in the AFM image.

If the large protrusions observed by AFM after fixation result from membrane protein aggregation, then the position of the fluorescence signal of the membrane protein after fixation should mostly correspond to the position of the large protrusion on the cell surface. To confirm this, we investigated whether the fluorescent signal of the membrane protein corresponded to the protrusion in the AFM image. To accurately superimpose the AFM image on the fluorescence images, we developed a method to stain MPMs with fluorescein isothiocyanate (FITC) and align the edges of the holes. Furthermore, we adopted stimulated emission depletion (STED) microscopy to determine the molecule's position as accurately as possible. Figure 4a and b show the images of the cell on the MPM with 3-μm holes obtained through AFM and fluorescence microscopy, respectively. Figure 4c shows the overlaid image of Figure 4a and b. Figure 4d and e show the cropped AFM images in which the contrast was adjusted superimposed on the original AFM image and the fluorescence image, respectively. Magnified images of the superimposed area in Figure 4e are depicted in Figure 4f. The localization of many E-cadherin signals appears to correspond to the protrusion in the AFM images (Figure 4f). Because there are many membrane proteins other than E-cadherin, large protrusions can be thought to be created by the aggregation of surrounding various kinds of membrane proteins. This result supports that the large protrusion in the AFM image after fixation was due to the aggregation of membrane proteins.

Discussion

This study demonstrated that the size of the protrusions on the cell surface observed by AFM is increased after treatment with three commonly used fixatives, PFA, GA, and MeOH. This was probably caused by the aggregation of the membrane proteins. Of the three fixatives used in this study, the effect of MeOH

was relatively weak and less significant than that of PFA and GA (Figure 2 and 3). These results can be explained by the difference in the fixation mechanism (Figure 5). Aldehyde fixatives, such as PFA and GA, directly create crosslinks between membrane proteins. In contrast, alcohol fixatives such as MeOH just remove water between proteins and precipitate them, so the aggregation produced by MeOH is thought to be looser than that of PFA or GA. We consider that the lower significant effect of MeOH as a fixative in the experiments of the nearest distance reflects this difference in the fixation mechanism.

This study showed that the fixative treatment extinguished the small protrusions and created large ones. We demonstrated that the aggregation of the membrane proteins caused these large protrusions through fluorescence experiments. However, another possible mechanism is that cortical actin polymerization slightly pushed the membrane out as in the beginning of the filopodia formation[49, 50]. Some protrusions may be created because of this reason, but it is unlikely that this mechanism produces all the protrusions presented on the entire cellular surface. Rather, the aggregation of actin filaments facilitates the aggregation of membrane proteins[51]. Therefore, it is most reasonable to assume that most of the large protrusions were created by the aggregation of membrane proteins by fixatives. The protrusions reported in this study are different from the previously reported cell surface structures, such as microvilli or microridges[57, 58], because these structures are much higher than the protrusions reported here (microvillus ~1 μm, microridge ~300 nm) and look very different from the protrusions in this study[52, 53].

Fixatives have been used in thousands of studies, and some have investigated the size of the clusters or nanoscale colocalization of membrane proteins using fixed cells. We suggest that readers are aware that nanoscale clusters and colocalization may include the effect of fixation. Researchers who observe nanoscale clusters also should be careful in interpreting their experimental results when using fixed cells. We recommend that researchers use living cells as much as possible to avoid the effect of fixation when investigating nanoscale clusters of colocalization. Or, if a lipid-only fixation method is developed in the future, it may be possible to achieve a more structure-preserving fixation. Thus, this study should be necessary for past and future nanoscale observations using fixed cells.

Methods

Cell sample preparation

The human colon cancer cell line DLD-1 was supplied by the Cell Resource Center for Biomedical Research, Tohoku University, Japan. The cells were cultured in the Dulbecco's modified Eagle's medium (Gibco) supplemented with 10% fetal bovine serum (Biosera) and 1% penicillin/streptomycin (Fujifilm Wako Pure Chemical Corporation). Microporous silicon nitride membranes (MPM, NH050D549 or NX5100CH3, Norcada) were fixed onto 35 mm-plastic dishes using double-sided tape with the membrane side facing down (Figure 1f). We placed the 10 μL of the cell suspension solution, which contained 5×10^3 cells, on the pocket that was on the reverse side of the MPM. The cell solutions were placed in a CO_2

incubator and were cultured for 2.5 days. For fluorescence imaging, we seeded 4×10^4 cells onto a 35-mm glass-bottom dish (Matsunami Glass) and cultured them for 2.5 days in the culture medium.

Fixation

The fixatives used in this study were 4% paraformaldehyde (PFA) (Fujifilm Wako Pure Chemical Corporation), 25% glutaraldehyde (GA) (1st grade, Fujifilm Wako Pure Chemical Corporation), and methanol (MeOH) (1st grade, Fujifilm Wako Pure Chemical Corporation). The samples were fixed using 4% PFA for 30 min at room temperature (RT), 2% GA in PBS for 1 h at RT, or cold 100% MeOH for 20 min at −20°C.

Atomic force microscopy (AFM) imaging

We fixed the cell-cultured MPM onto the MPM holder dish using a perfusion system (custom-made by Nagata Industry Co.) with the membrane facing up. The MPM was bathed in Leibovitz's L-15 medium (Thermo Fisher Scientific) supplemented with 1% penicillin/streptomycin (Fig. 1f). Then, the MPM holder dish was set on the stage of an inverted fluorescence microscope (Eclipse Ti2, Nikon) coupled to a JPK NanoWizard 4 BioAFM (Bruker). AFM imaging was performed using BL-AC40TS-C2 cantilevers (Olympus, spring constant approximately 0.1 N/m). We used the QI settings with following parameters: topography imaging: 2.5 × 2.5 or 0.5 × 0.5 μm scale, 64 × 64 pixels, Z-length 1 μm, setpoint 0.1 nN, speed 166 μm/s; imaging at the 100 × 100 nm scale: 64 × 64 pixels, Z-length 50 nm, setpoint 0.1 nN, speed 166 μm/s; for Young’s modulus measurement: 100 × 100 nm scale, 64 × 64 pixels, Z-length 2 μm, setpoint 0.1 nN, speed 166 μm/s.

AFM data analysis

JPK data processing software (ver. 7, Bruker) was used to process the AFM images (plain fitting degree 2, line levelling degree 3, median filter mask width 3, and tolerance 0.5), and they were exported as Tiff images with 512 × 512 pixels. These images were imported into a custom-made script written in MATLAB (MathWorks, available upon request). The area of the protrusions was determined, and the area or the nearest distance between protrusions was measured automatically (Figure S1). The area or the nearest distance distributions were plotted using Prism 7 (GraphPad Software). Young's modulus was calculated using JPK data processing, which employs a Hertz model for a triangular pyramid (angle 17.5°) fitted to the extended curves.

Fluorescence imaging

The cells were labelled using primary antibodies, which bind to the extracellular domain of E-cadherin (ab40772, Abcam) or EpCAM (14-9326-82, Thermo Fisher Scientific), and the following secondary antibodies: STAR RED goat anti-rabbit IgG (STRED-1002, Abberior) or STAR ORANGE goat anti-mouse IgG (STAR ORANGE-1001, Abberior). After culturing the cells on a 35 mm glass-bottom dish, we blocked with Blocking One (Nacalai Tesque) for 30 min at 37°C and subsequently incubated the cells using the primary antibody solution (1:500 dilution in the culture medium) for 30 min at 37°C. The cells were washed with warmed PBS and incubated with secondary antibody solution (1:500 dilution in the culture medium) for

30 min at 37°C. Then they were washed again with warmed PBS, and the culture medium was replaced with Leibovitz's L-15 medium (no phenol red) supplemented with 1% penicillin/streptomycin[54]. In the experiments in Figure 4, the E-cadherin was labelled using E-cadherin antibody (ab40772, Abcam) and fluorescence labelled secondary antibody (STRED-1002, Abberior) after AFM observation to avoid the detection of the antibody in AFM imaging.

For confocal imaging, we used the Abberior Expert Line (Abberior Instruments) equipped with an inverted microscope (IX83, Olympus). We used oil immersion 100x lends (NA. 1.3) and illuminated with 561 and 640 nm lasers. We acquired an image with a resolution of 50 × 50 nm per pixel. For STED imaging, we used the 2D STED mode. We acquired images with a resolution of 20 × 20 nm per pixel. 561 and 640 nm lasers were used for illumination, and 775 nm laser was used for depletion.

For time-lapse imaging, we set the small scan area (20 × 17 μm, 50 × 50 nm per pixel) and acquired images every 2 s. A 1/12.5 volume of 25% GA was added during time-lapse imaging by a perfusion system that has been customized for the dish holders (Figures 1f and g).

Fluorescence image analysis

We cropped the image of the cell and identified each spot using the ImageJ plug-in, Track Mate[55]. We set the size of the spots as 0.5 mm and the threshold at 0.2. We aligned the number of spots before and after fixation and then measured the nearest distance using the position information and a custom script made by MATLAB (R2020b, Simulink). Scatter plots were created using Prism 7 (GraphPad Software).

References

1. Sabatini DD, Bensch K, Barrnett RJ. Cytochemistry and electron microscopy. The preservation of cellular ultrastructure and enzymatic activity by aldehyde fixation. *J Cell Biol* **17**, 19-58 (1963).
2. Hopwood D. Cell and tissue fixation, 1972-1982. *Histochem J* **17**, 389-442 (1985).
3. Ramos-Vara JA. Principles and Methods of Immunohistochemistry. *Methods Mol Biol* **1641**, 115-128 (2017).
4. Kiernan JA. Formaldehyde, formalin, paraformaldehyde and glutaraldehyde: what they are and what they do. *Microscopy today* **1**, 8-12 (2000).
5. Eltoum I, Fredenburgh J, Myers RB, Grizzle WE. Introduction to the theory and practice of fixation of tissues. *Journal of Histotechnology* **24**, 173-190 (2001).
6. Matsuno A*, et al.* Electron microscopic observation of intracellular expression of mRNA and its protein product: technical review on ultrastructural in situ hybridization and its combination with immunohistochemistry. *Histol Histopathol* **15**, 261-268 (2000).
7. Habeeb AJ, Hiramoto R. Reaction of proteins with glutaraldehyde. *Arch Biochem Biophys* **126**, 16-26 (1968).

8. Molin SO, Nygren H, Dolonius L. A new method for the study of glutaraldehyde-induced crosslinking properties in proteins with special reference to the reaction with amino groups. *J Histochem Cytochem* **26**, 412-414 (1978).
9. Kim KW. Methanol fixation for scanning electron microscopy of plants. *Appl Microsc* **50**, 10 (2020).
10. Stanly TA*, et al.* Critical importance of appropriate fixation conditions for faithful imaging of receptor microclusters. *Biol Open* **5**, 1343-1350 (2016).
11. Tanaka KA*, et al.* Membrane molecules mobile even after chemical fixation. *Nat Methods* **7**, 865-866 (2010).
12. Shah JP, Kumaraswamy SV, Kulkarni V. Comparative evaluation of fixation methods after mandibulotomy for oropharyngeal tumors. *Am J Surg* **166**, 431-434 (1993).
13. Li Y*, et al.* The effects of chemical fixation on the cellular nanostructure. *Exp Cell Res* **358**, 253-259 (2017).
14. Pereira PM*, et al.* Fix Your Membrane Receptor Imaging: Actin Cytoskeleton and CD4 Membrane Organization Disruption by Chemical Fixation. *Front Immunol* **10**, 675 (2019).
15. Kuzmin AN, Pliss A, Prasad PN. Changes in biomolecular profile in a single nucleolus during cell fixation. *Anal Chem* **86**, 10909-10916 (2014).
16. Murk JL*, et al.* Influence of aldehyde fixation on the morphology of endosomes and lysosomes: quantitative analysis and electron tomography. *J Microsc* **212**, 81-90 (2003).
17. Zhou X*, et al.* Preservation of cellular nano-architecture by the process of chemical fixation for nanopathology. *PLoS One* **14**, e0219006 (2019).
18. Braet F, Rotsch C, Wisse E, Radmacher M. Comparison of fixed and living liver endothelial cells by atomic force microscopy. *Appl Phys a-Mater* **66**, S575-S578 (1998).
19. Mason JT, O'Leary TJ. Effects of formaldehyde fixation on protein secondary structure: a calorimetric and infrared spectroscopic investigation. *J Histochem Cytochem* **39**, 225-229 (1991).
20. Kim SO, Kim J, Okajima T, Cho NJ. Mechanical properties of paraformaldehyde-treated individual cells investigated by atomic force microscopy and scanning ion conductance microscopy. *Nano Converg* **4**, 5 (2017).
21. Liu BY, Zhang GM, Li XL, Chen H. Effect of glutaraldehyde fixation on bacterial cells observed by atomic force microscopy. *Scanning* **34**, 6-11 (2012).
22. Le Grimellec C, Lesniewska E, Giocondi MC, Finot E, Vie V, Goudonnet JP. Imaging of the surface of living cells by low-force contact-mode atomic force microscopy. *Biophys J* **75**, 695-703 (1998).
23. Schnell U, Dijk F, Sjollema KA, Giepmans BN. Immunolabeling artifacts and the need for live-cell imaging. *Nat Methods* **9**, 152-158 (2012).
24. Sinniah K, Paauw J, Ubels J. Investigating live and fixed epithelial and fibroblast cells by atomic force microscopy. *Curr Eye Res* **25**, 61-68 (2002).
25. Le Grimellec C, Giocondi MC, Pujol R, Lesniewska E. Tapping mode atomic force microscopy allows the in situ imaging of fragile membrane structures and of intact cells surface at high resolution.

Single molecules **1**, 105-107 (2000).

26. Drake B*, et al.* Imaging crystals, polymers, and processes in water with the atomic force microscope. *Science* **243**, 1586-1589 (1989).
27. Ohnesorge F, Binnig G. True atomic resolution by atomic force microscopy through repulsive and attractive forces. *Science* **260**, 1451-1456 (1993).
28. Fukuma T, Kobayashi K, Matsushige K, Yamada H. True atomic resolution in liquid by frequency-modulation atomic force microscopy. *Appl Phys Lett* **87**, 034101 (2005).
29. Fukuma T. Water distribution at solid/liquid interfaces visualized by frequency modulation atomic force microscopy. *Sci Technol Adv Mater* **11**, 033003 (2010).
30. Dufrene YF*, et al.* Imaging modes of atomic force microscopy for application in molecular and cell biology. *Nat Nanotechnol* **12**, 295-307 (2017).
31. Yamashita H, Taoka A, Uchihashi T, Asano T, Ando T, Fukumori Y. Single-molecule imaging on living bacterial cell surface by high-speed AFM. *J Mol Biol* **422**, 300-309 (2012).
32. Li M*, et al.* Progress of AFM single-cell and single-molecule morphology imaging. *Chinese Science Bulletin* **58**, 3177-3182 (2013).
33. Shibata M, Watanabe H, Uchihashi T, Ando T, Yasuda R. High-speed atomic force microscopy imaging of live mammalian cells. *Biophys Physicobiol* **14**, 127-135 (2017).
34. Allison DP, Mortensen NP, Sullivan CJ, Doktycz MJ. Atomic force microscopy of biological samples. *Wiley Interdiscip Rev Nanomed Nanobiotechnol* **2**, 618-634 (2010).
35. de Pablo PJ, Carrion-Vazquez M. Imaging biological samples with atomic force microscopy. *Cold Spring Harb Protoc* **2014**, 167-177 (2014).
36. Moloney M, McDonnell L, O'Shea H. Atomic force microscopy of BHK-21 cells: an investigation of cell fixation techniques. *Ultramicroscopy* **100**, 153-161 (2004).
37. Dufrene YF. Atomic force microscopy in microbiology: new structural and functional insights into the microbial cell surface. *mBio* **5**, e01363-01314 (2014).
38. Shibata M, Watanabe H, Uchihashi T, Ando T, Yasuda R. High-speed atomic force microscopy imaging of live mammalian cells. *Biophysics and physicobiology* **14**, 127-135 (2017).
39. White SH, Wimley WC. Membrane protein folding and stability: physical principles. *Annu Rev Biophys Biomol Struct* **28**, 319-365 (1999).
40. Vinothkumar KR, Henderson R. Structures of membrane proteins. *Q Rev Biophys* **43**, 65-158 (2010).
41. Erickson HP. Size and shape of protein molecules at the nanometer level determined by sedimentation, gel filtration, and electron microscopy. *Biological procedures online* **11**, 32-51 (2009).
42. Hutter JL, Chen J, Wan WK, Uniyal S, Leabu M, Chan BM. Atomic force microscopy investigation of the dependence of cellular elastic moduli on glutaraldehyde fixation. *J Microsc* **219**, 61-68 (2005).
43. Codan B, Martinelli V, Mestroni L, Sbaizero O. Atomic force microscopy of 3T3 and SW-13 cell lines: an investigation of cell elasticity changes due to fixation. *Mater Sci Eng C Mater Biol Appl* **33**, 3303-3308 (2013).

44. Yamane Y, Shiga H, Haga H, Kawabata K, Abe K, Ito E. Quantitative analyses of topography and elasticity of living and fixed astrocytes. *J Electron Microsc (Tokyo)* **49**, 463-471 (2000).
45. Sneddon IN. The relation between load and penetration in the axisymmetric Boussinesq problem for a punch of arbitrary profile. *Int J Eng Sci* **3**, 47-57 (1965).
46. Hertz H. Study on the contact of elastic bodies. *J Reine Angew Math* **29**, 156-171 (1882).
47. Kuznetsova TG, Starodubtseva MN, Yegorenkov NI, Chizhik SA, Zhdanov RI. Atomic force microscopy probing of cell elasticity. *Micron* **38**, 824-833 (2007).
48. Shafraz O, Xie B, Yamada S, Sivasankar S. Mapping transmembrane binding partners for E-cadherin ectodomains. *Proc Natl Acad Sci U S A* **117**, 31157-31165 (2020).
49. Mellor H. The role of formins in filopodia formation. *Biochim Biophys Acta* **1803**, 191-200 (2010).
50. Gat S, Simon C, Campillo C, Bernheim-Groswasser A, Sykes C. Finger-like membrane protrusions are favored by heterogeneities in the actin network. *Soft Matter* **16**, 7222-7230 (2020).
51. Gudheti MV*, et al.* Actin mediates the nanoscale membrane organization of the clustered membrane protein influenza hemagglutinin. *Biophys J* **104**, 2182-2192 (2013).
52. Kim HR, Jun CD. T Cell Microvilli: Sensors or Senders? *Front Immunol* **10**, 1753 (2019).
53. Pinto CS, Khandekar A, Bhavna R, Kiesel P, Pigino G, Sonawane M. Microridges are apical epithelial projections formed of F-actin networks that organize the glycan layer. *Sci Rep* **9**, 12191 (2019).
54. Cho KW, Morris DL, Lumeng CN. Flow cytometry analyses of adipose tissue macrophages. *Methods Enzymol* **537**, 297-314 (2014).
55. Tinevez JY*, et al.* TrackMate: An open and extensible platform for single-particle tracking. *Methods* **115**, 80-90 (2017).

Figures

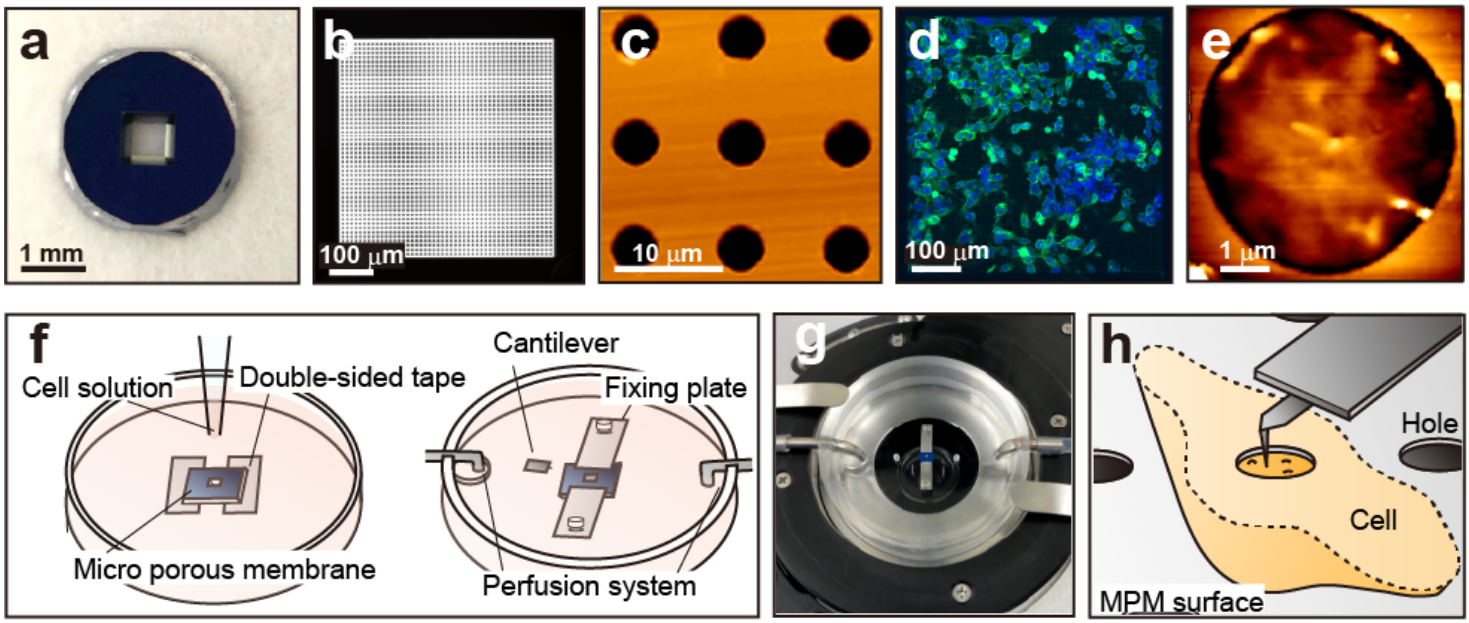

Figure 1

Microporous silicon nitride membrane (MPM) and its application to the cell surface observation in AFM imaging (a) Appearance of MPM (NH050D549, Norcada); frame size 2.6 × 2.6 mm, frame thickness 0.2 mm, membrane size 0.5 × 0.5 mm, membrane thickness 200 nm, hole diameter 5 μm, hole pitch 10 μm. (b) The transmitted light image of the membrane. (c) AFM image of the hole of the membrane. (d) Cultured DLD-1 cells on MPM. The cell membrane and nuclei are stained green and blue, respectively. (e) AFM image of the DLD-1 cell surface on the MPM hole. (f) Schematic diagram of the method for culturing and observing the cell surface using MPM. (g) Photo of the area around the sample. (h) Schematic diagram of the AFM observation of the cell surface using MPM.

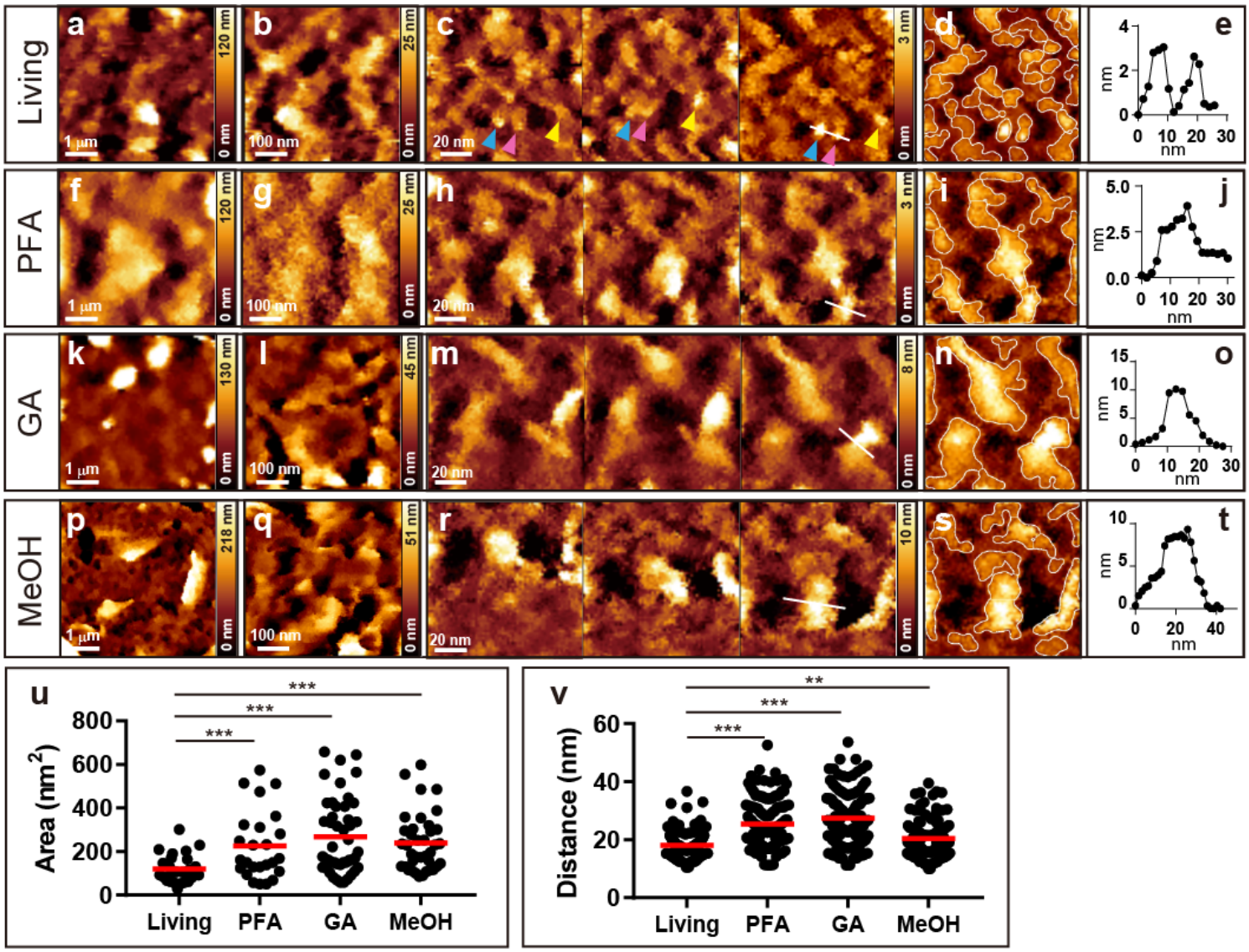

Figure 2

AFM images of the DLD-1 cell surface using MPM and the effect of the chemical fixation. (a) AFM image of the living DLD-1 cell surface using MPM in 2.5 × 2.5 μm scale. (b) 0.5 × 0.5 μm scale image. (c) Three consecutive images of 100 × 100 nm scale at the same position acquired every 1 min. Arrowheads of the same colours indicate the same protrusions. (d) Overlaid image of the third image in c with the boundary

of the recognized protrusion area (white line) through the auto-recognition tool. (e) Height profile along the line in c. (f) AFM image after treatment with 4% PFA in 2.5 × 2.5 μm scale. (g) 0.5 × 0.5 μm scale image. (h) Three consecutive images of 100 × 100 nm scale acquired every 1 min. (i) Overlaid image of the third image in h with the boundary of the recognized protrusion area (white line). (j) Height profile along the line in h. (k) AFM image after treatment with 2% GA in 2.5 × 2.5 μm scale. (l) 0.5 × 0.5 μm scale image. (m) Three consecutive images of 100 × 100 nm scale acquired at every 2 min. (n) Overlaid image of the third image in m with the boundary of the recognized protrusion area (white line). (o) Height profile along the line in m. (p) AFM image after treatment with cold 100% MeOH in 2.5 × 2.5 μm scale. (q) 0.5 × 0.5 μm scale image. (r) Three consecutive images of 100 × 100 nm scale acquired at every 2 min. (s) Overlaid image of the third image in r with the boundary of the recognized area (white line). (t) Height profile along the line in r. (u) Distributions of the protrusion area on the surface of living or fixed cells. Red bars indicate mean values. Asterisks (***) denote statistical significance ($p < 0.001$, t-test). (v) Distributions of the nearest distance between protrusions on the cell surface of living or fixed cells. Red bars indicate mean values. Asterisks (** or ***) denote statistical significance ($p < 0.01$ or $p < 0.001$, t-test).

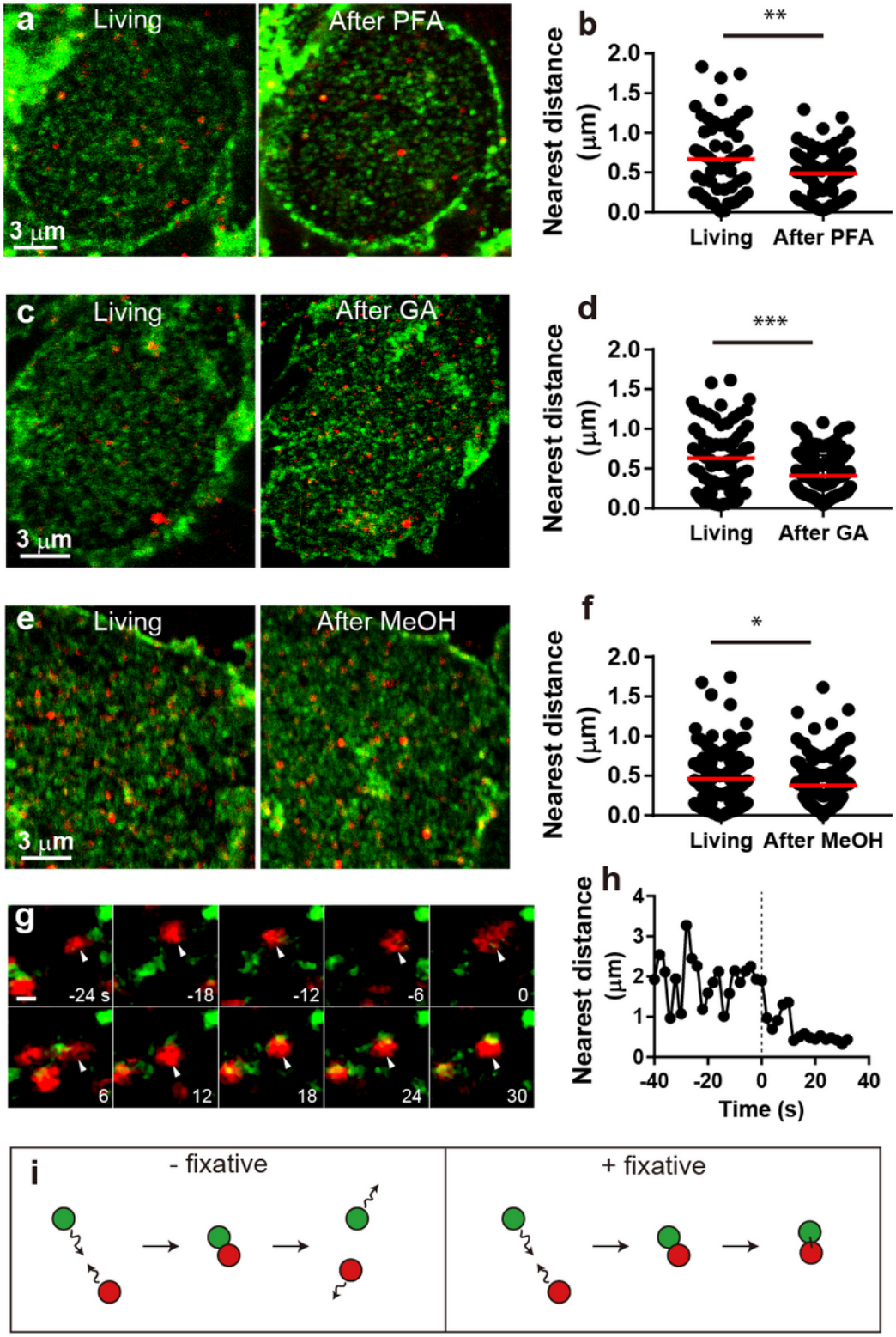

Figure 3

Nearest distance of two kinds of membrane proteins and the effect of fixatives. (a) Confocal images of E-cadherin (red) and EpCAM (green) before and after treatment with 4% PFA. (b) Distribution of the nearest distance. Red lines indicate mean values. Asterisks (**) denote statistical significance ($p < 0.01$, t-test). (c) Confocal images before and after treatment with 2% GA. (d) Distribution of the nearest distance. Red lines indicate mean values. Asterisks (***) denote statistical significance ($p < 0.001$). (e) Confocal images

before and after treatment with cold 100% MeOH. (d) Distribution of the nearest distance. Red lines indicate mean values. The Asterisk (*) denotes statistical significance ($p < 0.05$). (g) Time series during fixation. Arrowheads indicate the same molecule. The scale bar is 1 μm. 2% GA was added at 0 sec. (h) Time-lapse change of the nearest distance from the molecule indicated in g to EpCAM. The dotted line indicates the time point of GA addition. (i) Model of the behaviour of membrane proteins during fixation. Before adding fixatives, membrane proteins approach and move apart from each other. However, after adding a fixative, proteins cannot move apart once they make contact.

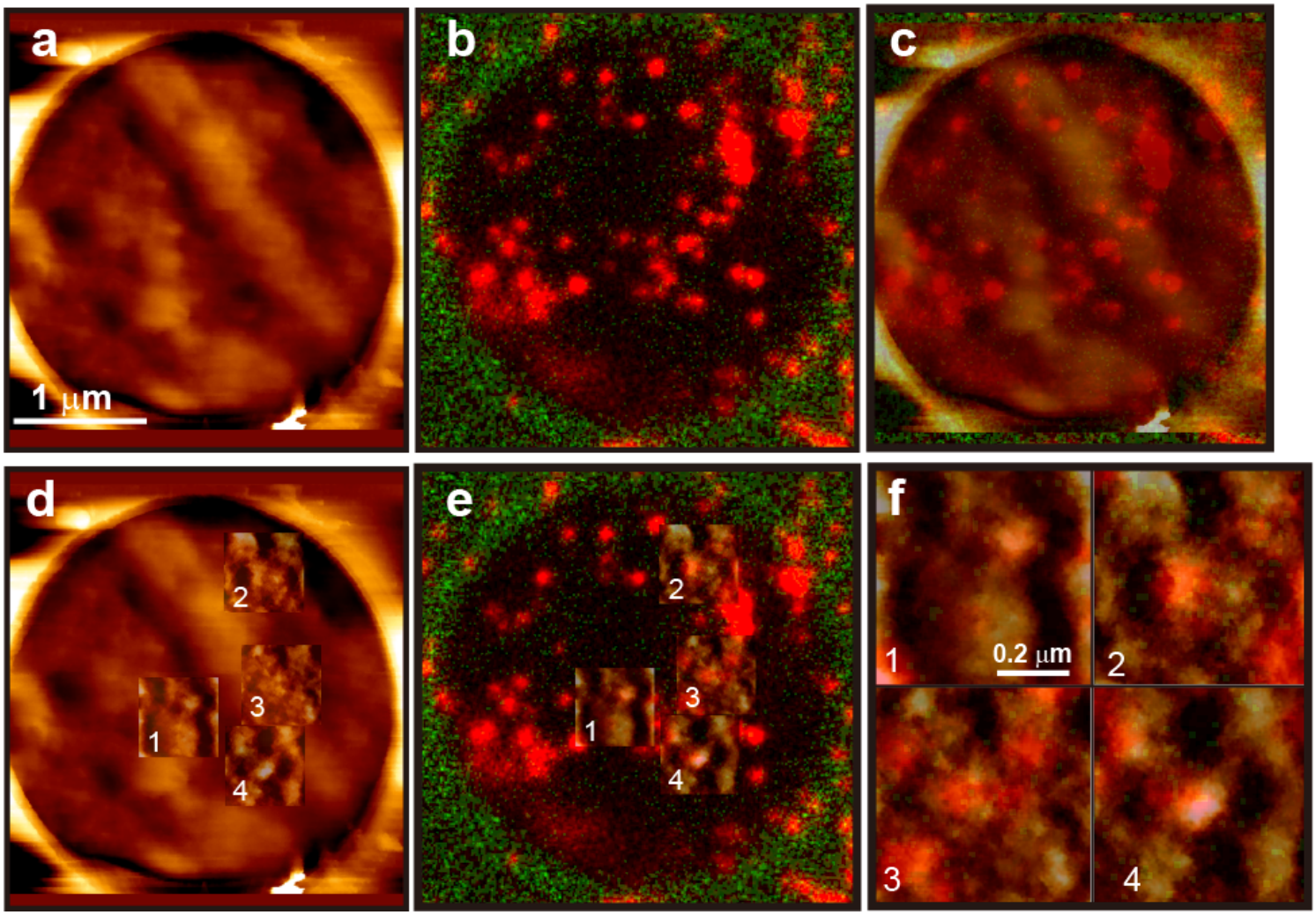

Figure 4

Correspondence of AFM and STED image. (a) AFM image of DLD-1 cell cultured on 3 μm MPM. (b) STED image of the same position and scale depicted on a. Red spots indicate the localization of E-cadherin. MPM is stained with FITC. (c) Superimposed image of AFM and fluorescence images. (d) Superimposed image of cropped and contrast adjusted AFM image and original AFM image. (e) Superimposed image of cropped AFM image and STED image. (f) Magnified overlayed image of e. Numbers correspond in e.

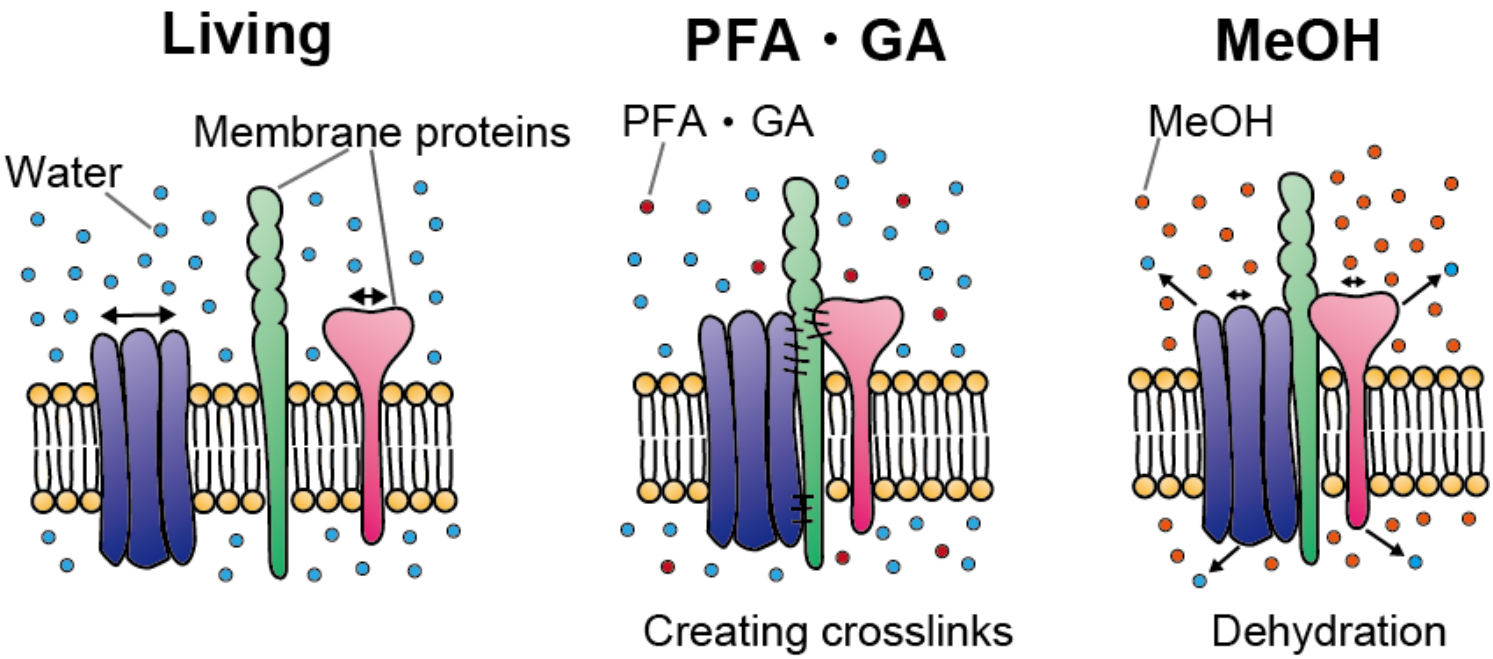

Figure 5

Model of the fixation mechanism of membrane proteins using aldehyde or alcohol fixatives. Aldehyde fixatives (such as PFA and GA) directly create crosslinks between membrane proteins. Thus the nearest distance between membrane proteins is thought to be close. In contrast, alcohol fixatives (such as MeOH) dehydrate and precipitate proteins. Therefore, it can be thought that the binding between membrane proteins is loose, and the nearest distances are not very close. This difference reflects the weak effect of MeOH in Figures 2 and 3.

Supplementary Files

This is a list of supplementary files associated with this preprint. Click to download.

- SupportingInformationIchikawaFukumaCommBiol.docx